

Received February 13, 2022, accepted March 1, 2022, date of publication March 10, 2022, date of current version March 24, 2022.

Digital Object Identifier 10.1109/ACCESS.2022.3158669

Performance Evaluation of 5G Millimeter-Wave-Based Vehicular Communication for Connected Vehicles

ZADID KHAN¹, SAKIB MAHMUD KHAN², (Senior Member, IEEE),
MASHRUR CHOWDHURY², (Senior Member, IEEE),
MIZANUR RAHMAN³, (Member, IEEE), AND MHAFUZUL ISLAM⁴

¹Walmart Supply Chain (Transportation), Bentonville, AR 72712, USA

²Glenn Department of Civil Engineering, Clemson University, Clemson, SC 29631, USA

³Department of Civil, Construction and Environmental Engineering, University of Alabama, Tuscaloosa, AL 35487, USA

⁴General Motors R&D, Warren Technical Center, Warren, MI 48092, USA

Corresponding author: Sakib Mahmud Khan (sakibk@clemson.edu)

This work was supported by the Center for Connected Multimodal Mobility (C²M²) (the U.S. Department of Transportation Tier 1 University Transportation Center) headquartered at Clemson University, Clemson, SC, USA.

ABSTRACT Due to the drastic increase in the volume of data generated by connected vehicles (CVs), future vehicle-to-infrastructure (V2I) applications will require a communication medium that offers high-speed and high bandwidth communication while maintaining reliability in high-mobility traffic scenarios. The 5G millimeter-wave (mmWave) can solve the communication issues related to V2I applications. However, the performance of the 5G mmWave for vehicular communication in high-mobility urban traffic scenarios is yet to be evaluated. This study presents a case study on assessing the performance of the 5G mmWave-based vehicular communication in such traffic scenarios. We have designed three realistic use cases for performance evaluation based on three challenges: dynamic mobility, increased CV penetration level, and V2I application specifications, such as data rate and packet size. We have also created a simulation-based experimental setup using a microscopic traffic simulator (SUMO) and a communication network simulator (ns-3) to simulate the use cases. We have used delay, packet loss, throughput, and signal-to-interference-plus-noise ratio (SINR) as the communication performance evaluation metrics. Our analyses found that the CV penetration level is the primary determinant of the performance of the 5G mmWave. Moreover, once the data rate is increased by a factor of 40, delay and packet loss increase by factors of 6.8 and 2.8, respectively.

INDEX TERMS Connected vehicle, 5G, millimeter-wave, communication, vehicle-to-infrastructure, V2I.

I. INTRODUCTION

A. BACKGROUND

Connected vehicles (CVs) are an integral part of the transportation cyber-physical systems (CPS). Numerous safety, mobility, and environmental benefits can be achieved through CV applications [1]. The communication technologies used for vehicular networks include the widely adopted Wireless Access in Vehicular Environments (WAVE/IEEE 802.11p), 4G, LTE, Cellular vehicle-to-everything (C-V2X), and 5G [2]. As identified in previous literature, the advantages of 5G over 4G and LTE includes increased spectrum allocation, improved capacity to aggregate simultaneous users within the coverage area, availability of directional beamforming anten-

The associate editor coordinating the review of this manuscript and approving it for publication was Derek Abbott¹.

nas, highly increased bit rates within increased proportions of the 5G coverage areas, and lower infrastructure cost [3]. Researchers have increasingly shown more interest in spectrums higher than 6 GHz to improve communication network reliability and throughput in the transportation CPS [4], [5]. The frequencies under 6 GHz are already allocated to various LTE bands [6]. Higher data throughput can be supported by the unused spectrums above 6 GHz for the increasing number of CVs in the future. The term ‘mmWave’ in the ‘5G mmWave’ refers to the spectrum corresponding to wavelengths between 1 and 10 millimeters [7]. Compared to LTE, the carrier frequency of the 5G mmWave allows for increased data rates while reducing the communication latency [8]. This inherent capacity offered by the 5G mmWave for both backhaul links (within multiple base stations) and access links (within the base station and end-users) can support the

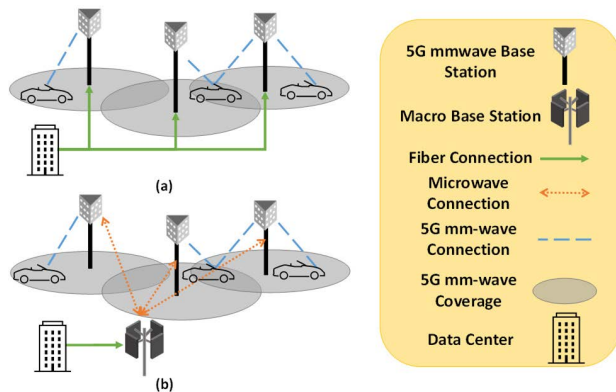


FIGURE 1. 5G mmWave network in urban environment.

CV environment [9]–[12]. The coverage area of mmWave communication is limited; however, extending the coverage area through multi-hop cooperative relay networks can significantly enhance communication network performance [13]. The wireless network operators increase the number of cell towers with reduced cell coverage areas to reduce interference and use cooperative multiple-input-multiple-output (MIMO) antennas at the receiver and sender end to compensate for the reduced cell coverage through improved relaying [3]. Future 5G mmWave based deployment will contain a high number of cell towers suitable for the future CV environment where an unprecedented number of CVs will demand multi-gigabit/second data transmission to support different CV applications.

CVs (both human-driven and automated vehicles) can run various data-intensive applications, such as in-vehicle infotainment systems [14] or sensor data sharing [15]. Figure 1 shows a conceptual 5G mmWave enabled CV scenario where a data center is connected with the mmWave base station either: (a) directly with a fiber-optic network or (b) via macro base stations. Multiple mmWave base stations can have overlapping regions to serve the high number of CVs if needed. The macro base stations operate at lower frequencies (below 6 GHz) to offer higher wireless communication coverage.

B. MOTIVATION

5G technologies have been deployed commercially in many locations across the world [16]. However, one of the 5G technologies, the 5G mmWave, is still in the development phase, and its application feasibility to roadway traffic is an important research area. The performance of the 5G mmWave base stations and the associated performance metrics for various roadway traffic scenarios is still an evolving research area. The initial phase of deploying any technology should include a thorough evaluation of the technology using simulation studies, identifying potential challenges, and finding the solutions to these challenges. This study was conducted to evaluate the efficacy of the 5G mmWave in different challenging roadway traffic scenarios in a simulation environment, which can provide valuable lessons that

could be used in the 5G mmWave experiments in a real-world roadway traffic scenario. Our study will support the future 5G mmWave integration in different connected vehicle applications.

C. CONTRIBUTIONS

Our contribution in this simulation-based study is providing performance data of 5G mmWave for V2I communication considering three specific challenges: dynamic mobility of CVs, different CV penetration levels with changing maximum speeds (which is the same as the posted speed limit in a corridor), and CV application requirements that correspond to variable data rate and packet size. In the first use case, we evaluate one 5G mmWave base station's performance for varying maximum speed of CVs, keeping the other factors (CV penetration level, application data rate, and packet size) constant. To quantify the relationship between CV mobility and the performance of the 5G mmWave communication (the second use case), we evaluate the performance of a 5G mmWave base station with varying numbers of CVs, keeping the other factors (maximum speed, application data rate, and packet size) constant. In the third use case, we evaluate one 5G mmWave base station's performance for variable data rate and packet size, keeping the other factors (maximum speed and CV penetration level) constant. We have also selected a baseline technology (WAVE/IEEE 802.11p) for comparison with the 5G mmWave. This study will also provide motivation for developing new connected vehicle applications that can benefit from 5G mmWave.

D. OUTLINE

In the rest of the paper, we first review the literature on the status of 5G and the use of 5G for vehicular communications. Section III describes the three use cases developed to evaluate the 5G mmWave performance. Sections IV and V describe the experimental setup for simulating the use cases and performance evaluation metrics used in this study, respectively. Section VI presents the evaluation results obtained by simulating the use cases. Section VII discusses the conclusions based on the results obtained in Section VI. Section VIII provides recommendations for future research related to the 5G mmWave-based vehicular communication.

II. LITERATURE REVIEW

The telecommunications industry and academia are involved in research to find technologies to support higher data rate and enhance spectral communication efficiency. Since the early 1980s, every ten years, a new generation of emerging communication technologies has replaced the old one: first-generation analog frequency modulation (FM) cellular systems in 1981, second-generation (2G) digital technology in 1992, 3G in 2001, and LTE-A in 2011 [17]. The 3rd generation partnership project or 3GPP consists of seven standard organizations, and they are responsible for creating the 5G new radio (NR) standards. The 3GPP published the

first complete set of 5G NR standards in 2017 in Release 15 [18]. Further updates on 5G NR standards will be published in Releases 16 and 17, which will include vehicle-to-everything (V2X) application layer services [19]. In the US, the telecommunication industry, including AT&T, Verizon, and Sprint, have deployed 5G as a fully operational network in major cities, such as Atlanta, Boston, New York, Chicago, San Francisco, and Houston [16].

The barriers to reliable wireless communication for CV applications include dynamic network topology of vehicular communication due to high vehicle mobility and frequent data link disconnections [20], cross-channel interferences and consequent packet drops in adjacent channels [21], and increased channel access delays [22]. The 5G networks are expected to expand and support various use cases, such as enhanced Mobile Broadband (eMBB), Ultra-Reliable Low-Latency Communication (URLLC), and Massive Machine Type Communication (MMTC). The eMBB is designed for the high data rate mobile broadband services, which require seamless data access both indoors and outdoors. The URLLC is designed for applications with stringent latency and reliability requirements in highly mobile vehicular communications to enable the CV network. The MMTC supports a vast number of devices that sporadically generate a small amount of data.

Many recent studies have shown that the 5G mmWave can be applicable for connected vehicles because of its high communication bandwidth with a gigabit/sec data rate and low latency communication delay [9]–[12]. These studies focus on specific aspects of the 5G mmWave based V2X communication, such as 3D beam alignment strategies [9], software-defined networking-based ecosystems [10], content dissemination methods for enhanced V2X (eV2X) services [11], and propagation channels for vehicle-to-vehicle (V2V) communication [12]. Moreover, end-to-end 5G network slicing can enable mmWave communication for vehicular networks [23]. Dehos *et al.* have identified mmWave as the primary technology for next-generation communication [24]. Mastrosimone and Panno have studied hybrid mmWave and LTE access links' performance and compared the hybrid system against pure LTE-based access links [25]. They have found CVs can achieve increased throughput of 33% using the hybrid mmWave and LTE access links compared to solely using LTE scenario [25]. Mezzavilla *et al.* (2018) evaluated LTE and 5G mmWave communication with a single mobile node [26]. In a real-world experiment conducted by Kim (2019), the author used mmWave for V2V communication on a university campus and on city roads with different permitted vehicle speeds. Due to the real-world environment, frequent disconnections occurred, and the inter-vehicle connectivity was impacted by the vehicles' speed variations. However, sufficient throughput was maintained to exchange large volume of data through the V2V connectivity. In another study conducted by Giordani *et al.* (2017), the authors developed a mathematical model to perform connectivity analysis in mmWave-based vehicular networks [27]. Based on their anal-

ysis, Giordani *et al.* (2017) found the mean data throughput at different vehicle speeds remains the same with 5G mmWave.

As discussed above, no previous study quantified the 5G mmWave communication performance for different use cases considering dynamic mobility of CVs, different CV penetration levels with changing maximum speeds, and CV application requirements that correspond to variable data rate and packet size. Our study aims to address these research gaps and provide a simulation-based performance evaluation of the 5G mmWave for V2I applications in an urban roadway corridor. The purpose of our study is to evaluate the 5G mmWave communication medium that offers high bandwidth while maintaining reliability in high-mobility traffic scenarios. Our multi-vehicle traffic scenario testing is a more realistic extension of an earlier study conducted by Mezzavilla *et al.* (2018). Also, we demonstrated the comparison of mmWave communication with another widely studied communication option, i.e., WAVE/IEEE 802.11p.

III. USE CASES AND BASELINE TECHNOLOGY

Here we discuss the three use cases to evaluate 5G mmWave communication and the baseline technology, WAVE/IEEE 802.11p, whose performance is compared against the 5G mmWave.

A. USE CASES

To evaluate the efficacy of the 5G mmWave, we have selected an urban arterial (Woodruff Road), in Greenville County, South Carolina, US. Literature suggests that a 5G mmWave base station can cover a distance of 500m [8], so we have chosen a portion of the corridor (~500m) and considered one 5G mmWave base station. We use a microscopic traffic simulator (i.e., Simulation of Urban Mobility or SUMO) to model the corridor and simulate traffic flow through the corridor. We simulate downlink data traffic, where the remote host sends synthetic data packets with a specific packet size and bit rate, and the CVs receive the data while in motion, which is a V2I application and an eMBB use case of 5G. It is envisioned that one 5G mmWave base station can deliver 10 Gbps peak throughput [8], which is very useful when many users are running multiple high data rate applications. Our goal is to study the 5G mmWave communication performance for traffic scenarios with multiple CVs on the road network. This study will simulate multiple CVs running applications that need to download data at a high data rate while moving at high speed through the corridor. Figure 2 presents the roadway section we have simulated in this study.

We have mentioned three factors (high CV penetration level, dynamic mobility, and CV application requirements) that create challenges for the 5G mmWave-based vehicular communication. Based on these factors, we have designed three use cases to evaluate the performance of the 5G mmWave. We have also selected a baseline technology for comparison. The description of the three use cases and baseline technology is described here.

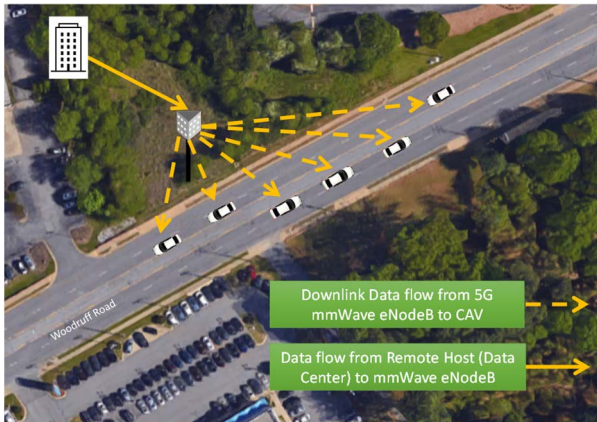


FIGURE 2. CV application data flow (downlink) using 5G mmWave eNB.

- 1) Use Case 1: CVs represent high-mobility nodes, which will make the communication between CVs and the 5G mmWave base stations challenging and often unreliable. This study evaluates the effect of CV mobility on the 5G mmWave communication performance for V2I applications. Here, CV mobility refers to the dynamic movement of CVs, which can be expressed using CV speed. The 5G mmWave can use any high-frequency spectrum above 24 GHz, decreasing communication reliability in high-mobility scenarios. In this use case, we evaluate one 5G mmWave base station's performance for varying maximum speed (35mph, 45mph, 55mph) of CVs, keeping the other factors (CV penetration level, application data rate, and packet size) constant. These constant values are: CV penetration level = 20 CVs, application data rate = 250 Kbps, and packet size = 256 bytes. For arterials, the three speeds mentioned above represent typical speed limits.
- 2) Use Case 2: In an urban roadway condition, many CVs may communicate with the backend infrastructure through the 5G mmWave base stations. The number of base stations needed will depend on the penetration of CV traffic on the roadway. As such, the number of CVs is an essential factor. In use case 2, we evaluate the performance of one of the 5G mmWave base stations for varying numbers of CVs (20, 40), along with altering the maximum speed of CVs (35 mph, 55 mph), keeping the other factors (maximum speed, application data rate, and packet size) constant. This experiment can be used to quantify the relationship between CV mobility and the performance of the 5G mmWave communication.
- 3) Use Case 3: The primary purpose of deploying the 5G mmWave base stations is to support applications with high bandwidth requirements. However, the uplink and downlink data rates between the CVs and the 5G mmWave base station will vary depending on application specifications. Moreover, the data packet size may also vary depending on the application. In use case 3, we evaluate one 5G mmWave base station's perfor-

mance for variable data rate (250 Kbps, 10 Mbps) and packet size (256 bytes, 1024 bytes), keeping the other factors (maximum speed and CV penetration level) constant. These constant values are: CV penetration level = 20 CVs, and maximum speed = 45 mph.

B. BASELINE TECHNOLOGY

We have selected the WAVE/IEEE 802.11p standard-based communication as the baseline technology. It is an established standard for vehicular communication that uses the 5.9 GHz spectrum, and significant research has been conducted to demonstrate its feasibility using simulations and field evaluations [28]. According to the federal communications commission (FCC), 5.9 GHz band will be used for indoor WiFi and C-V2X communication [29]. The C-V2X technology is developed using the Release 16 of the 3GPP standard for cellular communication, and it uses the 5.9 GHz spectrum for direct communication. The direct communication mode of C-V2X is called the 5G new radio (NR) sidelink. Although C-V2X is an emerging technology, initial studies have shown that the performance of C-V2X technology using 5.9 GHz is very similar to the performance of WAVE/IEEE 802.11p technology [30]. That is why we have selected WAVE/IEEE 802.11p for benchmarking in this study.

IV. EXPERIMENTAL SETUP

The details of the experimental setup for both 5G mmWave and WAVE/IEEE 802.11p are discussed in this section.

A. 5G mmWave SETUP

In this study, we use the network simulator, ns-3 [31] and the microscopic traffic simulator, SUMO [32]. Using ns-3, we model the communication between the CVs and the network infrastructure for the experimental setup. It is necessary to model the channel characteristics in a network device. To simulate the 5G mmWave communication in ns-3, we have used the mmWave module developed by the New York University (NYU) Wireless Group and the University of Padova [26]. The mmWave module can simulate a wide range of frequencies (i.e., 6 ~ 100 GHz) for 5G communication. The 5G mmWave module architecture is built upon the ns-3 LTE module (LENA), which uses the evolved packet core (EPC) network for LTE communications [33]. All layers in the 5G mmWave module from the network layer and above are identical to the LENA module. However, the mmWave PHY and MAC layers are explicitly designed for mmWave communication.

We create multiple "MmWaveUeNetDevice" objects in ns-3, representing the mmWave user equipment (UE) network devices to simulate multiple CVs. We also create one "MmWaveEnbNetDevice" object in ns-3 to simulate the radio stack in the mmWave base station (evolved Node B or eNB) [26]. All parameters related to the 5G mmWave simulation modeling are given in Table 1. The 5G mmWave eNB and other communication infrastructure, such as a data center working as a remote host, will have a constant position

TABLE 1. Consideration for wireless communication of CVs.

Wireless Communication Option	Considerations
5G mmWave	Frequency Band: 73 GHz Packet Size: 256 bytes, 1024 bytes Data Rate: 250 Kbps, 10 Mbps Blockage Model: Enabled Fading Model: Small-scale Fading PHY layer: Hybrid Automatic Repeat Request (HARQ) based retransmission MAC Layer: Round Robin Scheduler
WAVE/IEEE 802.11p	Frequency Band: 5.9 GHz Packet Size: 1024 bytes Data Rate: 250 Kbps Propagation Loss Model: Friis Fast Fading Model: Nakagami-m Routing Protocol: Ad hoc On-Demand Distance Vector (AODV) routing Transmission and Receiving Gain: 20 dBm (0.1 Watts)

mobility model. For the moving nodes or CVs, we have used the waypoint-following mobility model. We use SUMO to generate the trace file containing the CVs' motions, such as a CV's position, speed, and timestamp of data capture. The trace file is combined with the waypoint-following mobility model in ns-3 to model CV mobility in the network simulator. The network simulation generates several output files, which are post-processed to extract the evaluation metrics, such as throughput, delay, packet loss, and signal-to-interference-plus-noise ratio (SINR). The ns-3 simulation generates raw output files related to the radio link control (RLC) protocol and packet data convergence protocol (PDCP). The PDCP Tx and Rx files are packet traces that contain the information about each transmitted and received data packet during the simulation. The packet traces are post-processed to extract the packet information, along with timestamps and signal power. The packet information is used to generate output based on the selected evaluation metrics, which will be discussed in the following subsection. The findings presented in this paper have been obtained by running the ns-3 simulation for a short interval of 30 seconds due to the computational requirements of the 5G mmWave simulations.

Our approach to communication network simulation with network simulator (ns-3 and its predecessor ns-2) has been a widely accepted strategy for designing and validating network protocols in the industry and academia for a long time [26]. The outputs generated from the ns-3 simulator have been accepted to be reliable for representing the real-world network performance [26], [34], [35]. The 5G mmWave module's channel model used in the ns-3 simulation has been validated with real-world data [36]. The details of the 5G mmWave setup, WAVE/IEEE 802.11p setup, and performance metrics are given in the following subsections.

1) 5G mmWave CHANNEL CHARACTERISTICS

The first part of mmWave modeling is channel characteristics modeling. We have used the NYU statistical model as the propagation path loss model in this study [26]. This propagation model uses two separate equations for path loss considering line-of-sight (LOS) and non-line-of-sight (NLOS)

scenarios [26]. The communication channel matrices (i.e., beamforming vectors) are pre-generated and updated periodically (every 100 ms) to reduce computation burden during simulation while considering large-scale and small-scale fading. This model also assumes blockages, as it overlays the statistical channel model with the blockage model in ns-3 and chooses the appropriate propagation path loss model. This propagation model has been calibrated for two frequencies: 28 GHz and 73 GHz. Mobile network operators currently own the 28 GHz spectrum, so it is not a free spectrum that can be used for vehicular communication [19].

Moreover, a higher frequency is desirable because it achieves higher throughputs and data rates, which is the focus of this study. The channel model also calculates multipath interference by using an interference computation scheme. Each multipath communication link is associated with beamforming vectors, and these vectors are used to calculate the interference. The beamforming vectors consist of several parameters, such as the departure angle and arrival angle. The error model in the mmWave module follows the LTE LENA error model [33].

2) 5G mmWave PHY AND MAC LAYER

Here, we describe the PHY and MAC layer properties of the mmWave module used in our simulation. The mmWave module uses a time division duplexing (TDD) frame and subframe structure following the LTE standards. However, TDD allows the module to allocate the control and data channels within the subframe in a flexible way. It also uses the hybrid automatic repeat request (HARQ) based retransmission, which helps to do fast retransmission of data packets and increases the probability of successful decoding at the data receiving end. The HARQ model is combined with channel beamforming to ensure that all transmitted packets are received. In the MAC layer, time division multiple access (TDMA) is used as the default scheme because of analog beamforming. Analog beamforming refers to the transmitter antenna arrays aligning with the receiver antenna arrays to maximize the directional gain. Analog beamforming is one type of directional transmission. The adaptive modulation and coding (AMC) mechanism is used in our simulations, which uses the channel quality indicators (CQI) to update the modulation and coding. The MAC scheduler is based on a variable transmission time interval (TTI). This study uses the round-robin scheduler, which uses the orthogonal frequency division multiplexing (OFDM) and assigns OFDM symbols to flows in a round-robin order [26].

3) THE 5G mmWave INTERNET STACK (TCP/IP)

The remaining layers, including the internet stack (i.e., TCP/IP protocol suite), follow the LTE LENA module [26]. The "MmWaveHelper" object in ns-3 is used to model the 5G mmWave stack in ns-3 simulation (e.g., channel, PHY, MAC). A UE (i.e., CV) is attached to the closest eNB at the start of the simulation. As we are interested in an end-to-end

transmission scenario, a packet gateway (PGW) node connected to the backhaul LTE core network is also created. The positions of the eNB are fixed, and the UE mobility model is derived from the trace file generated through SUMO using the “Ns2mobilityhelper” object. We have used UDP unicast transmission in this study since we want to achieve higher throughput at the cost of lower reliability.

B. WAVE/IEEE 802.11P SETUP

To model WAVE/IEEE 802.11p communication in ns-3, we have used the WAVE module developed following the IEEE 802.11p, IEEE 1609, and SAE J2735 standards. We have used the WAVE/IEEE 802.11p module provided in ns-3 [37]. The WAVE/IEEE 802.11p module in ns-3 focuses on the multi-channel coordination layer and MAC layer. The PHY layer is similar to the IEEE 802.11 PHY layer. The WAVE module in ns-3 allows simulation of the vehicular ad-hoc network (VANET) scenarios and network performance assessment for different 802.11p MAC/PHY characteristics, propagation loss models, and data routing methods in realistic roadway scenarios. ns-3 includes a VANET example that uses 802.11p communication [38]. In [38], the example simulation runs for ten simulated seconds with 40 nodes (i.e., 40 CVs). All nodes transmit 200-byte basic safety messages ten times per second at 6 Mbps with continuous access to a 10 MHz Control Channel (CH) for all data traffic. Since the example scenario is similar to our scenario with an addition of a base station or a roadside unit (RSU), we have used the WAVE module in ns-3 to simulate the VANET scenario for our study.

The propagation loss depends on two significant factors: the distance between the communicating nodes and multipath fading. We use the Friis propagation loss model to account for path loss due to distance and the Nakagami-m fast fading loss model to account for the path loss due to multipath fading [39]. For simulation, we use 20 dBm (equivalent to 0.1 Watts) transmission power. The choice of routing protocol is important for scenarios selected in this study since the routing protocol directly affects the network’s quality of service. In terms of routing protocol, we have used the ad-hoc on-demand distance vector (AODV) protocol, which is one of the most widely used routing protocols for ad-hoc mobility-related scenarios [37], [40]–[42]. A recent study has shown that the AODV routing protocol provides a higher packet delivery ratio, throughput and normalized routing load than other routing protocols for different IEEE 802.11p VANET scenarios in terms of vehicular densities and speeds [43]. Similar to the 5G mmWave scenario, we have used a waypoint-following mobility model in this case. The same trace files as the mmWave cases are used for node mobility. The RSU node is treated as a stationary node with a fixed position. The UDP unicast transmission mode is used to send the data packets since it offers higher maximum throughput than the UDP broadcast mode. We have used the flow monitor in ns-3, which monitors the packet flow between the communicating nodes [44]. All the relevant parameters

TABLE 2. 5G mmWave PDCP layer statistics from simulation.

TX/RX	Sim. Time (sec)	Cell ID	RNTI	Packet size (bytes)	Delay (ns)
Tx	0.044818	1	9	1054	
Rx	0.044837	1	1	1054	863166
Tx	0.044923	1	10	1054	
Rx	0.045008	1	2	1054	928646
Tx	0.045028	1	11	1054	
Tx	0.045134	1	12	1054	
Tx	0.045239	1	13	1054	
Tx	0.045345	1	14	1054	
Rx	0.045446	1	8	1054	733686
Tx	0.04545	1	15	1054	

related to simulating WAVE/IEEE 802.11p in ns-3 are presented in Table 1.

V. PERFORMANCE EVALUATION METRICS

The details of performance evaluation metrics for both 5G mmWave and WAVE/IEEE 802.11p are discussed in this section.

A. METRICS FOR 5G mmWave

In ns-3, the 5G mmWave module is configured to output the aggregate statistics of the PDCP and RLC layer for all UEs (CVs) and the eNodeB (eNB). The aggregate output files contain the statistics related to all data packets transmitted from and received by UEs and eNBs during the simulation using 5G mmWave communication. Since PDCP and RLC files contain similar information, we only consider the PDCP output files. Table 2 contains a snapshot of the data available in the PDCP output file. Here, the initial three columns represent the type of packet (transmitted or received), simulation time and ID of the cell tower or eNB, respectively. We only have one eNB in simulation, so all packets originate from cell 1. The fourth column represents RNTI (radio network temporary identifier). RNTI is assigned based on the ID assignment method in the 5G NR standard, and it is the ID of the individual CVs or UEs in simulation. The fifth and sixth column represents the packet size of the transmitted or received packet and the delay information, respectively. Only Rx packets contain delay information. For Tx packets, there is no delay information. The evaluation metrics used in this study are average delay, throughput, packet loss, and SINR, as discussed in the following. SINR is a direct output from 5G mmWave simulation in the RX packet trace.

- 1) **Average delay:** For all Rx packets in Table 2, there is a value on the delay column. Therefore, we filter data from the table using the ‘TX/RX’ column name for Rx packets and take an average of the ‘Delay’ column to calculate the average delay for all CVs. Let us assume that the total number of Rx packets is n and the delay for the i^{th} packet is D_i . The delay is calculated using (1).

$$Delay = \frac{\sum_{i=1}^n D_i}{n} \quad (1)$$

- 2) **Throughput:** Throughput is also calculated using data about simulation time and packet size, and a snapshot of the data is shown in the second column

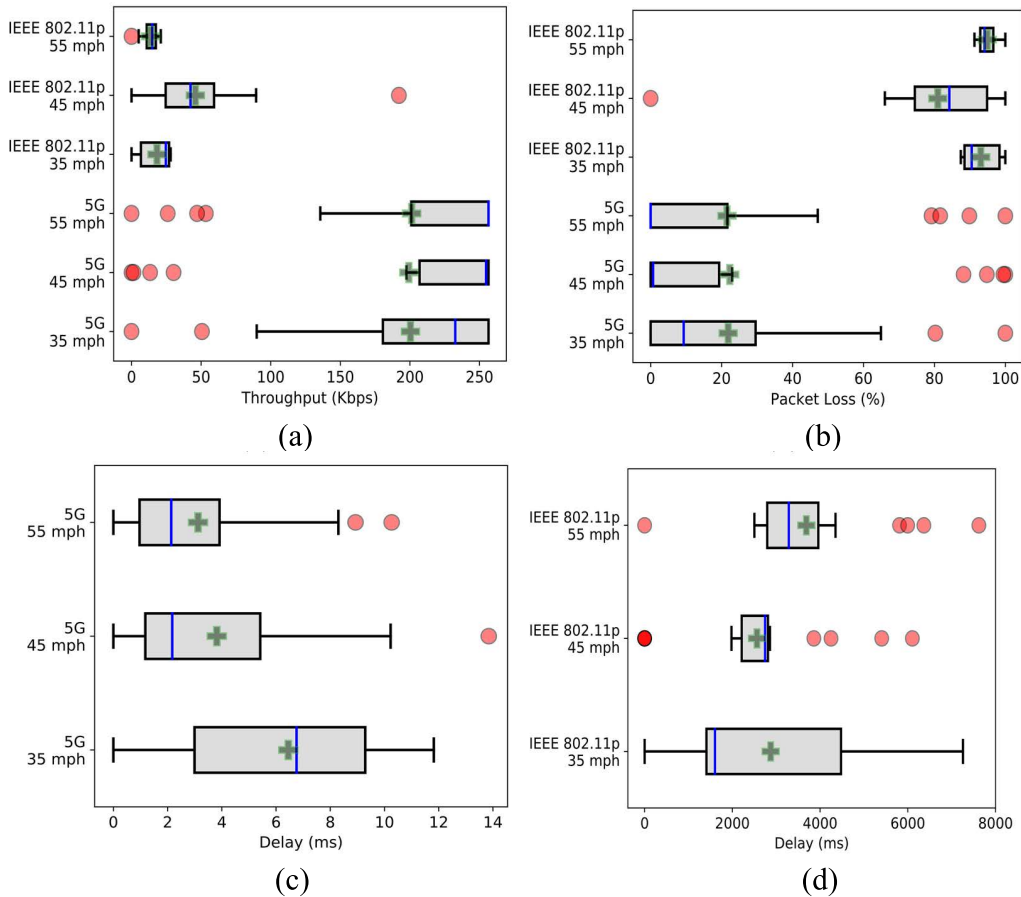


FIGURE 3. 5G mmWave performance for use case 1 and comparison with WAVE/IEEE 802.11p. (+ = sample mean): (a) throughput; (b) packet loss; (c) delay related to 5G; and (d) delay related to WAVE/IEEE 802.11p.

(Sim. Time (sec)) and fifth column (Packet size) of Table 2. The base station or eNB continuously transmits data to the different UEs (CVs), so we consider throughput as the rate of successful data transmission from the eNB to the CVs. Let us assume that the total number of Tx packets is m , the total number of Rx packets is n , the simulation timestamp of transmitting the i^{th} Tx packet is St_i , the simulation timestamp of receiving the i^{th} Rx packet is Sr_i , and the packet size of the i^{th} Rx packet is P_i . Therefore, the average throughput can be calculated using (2). The average throughput will be less than or equal to the transmission data rate of the eNB, which is a parameter in simulation.

$$Throughput = \frac{\sum_{i=1}^n 8P_i}{Sr_n - St_1} \quad (2)$$

3) **Packet Loss:** Packet loss means the percentage of packets sent by the eNB that were not received by the intended UEs or CVs. Let us assume that the number of Tx packets is m , and the number of Rx packets is n . Therefore, packet loss is calculated using (3).

$$PacketLoss = \frac{m - n}{m} \quad (3)$$

4) **SINR:** SINR can be calculated directly from one of the output files generated by the ns-3 5G mmWave simulation, which is the Rx packet trace file. In the Rx packet trace, SINR is the ratio of the incoming signal's power and the sum of the interference signal power from other objects and the noise power.

B. METRICS FOR BASELINE WIRELESS TECHNOLOGY (WAVE/IEEE 802.11P)

For WAVE/IEEE 802.11p scenarios (with which the 5G mmWave was compared), we have used the flow monitor in ns-3, which monitors the packet flow between the communicating nodes. Flow monitor provides specific output values for each flow in the simulation. Here, a flow is defined as a stream of data between two unique nodes. The output measures provided by the flow monitor, which we have used in our calculation, are given below:

- timeFirstTxPacket: when the first packet in a flow was transmitted
- timeLastTxPacket: when the last packet in a flow was transmitted
- timeFirstRxPacket: when the first packet in a flow was received by an end node

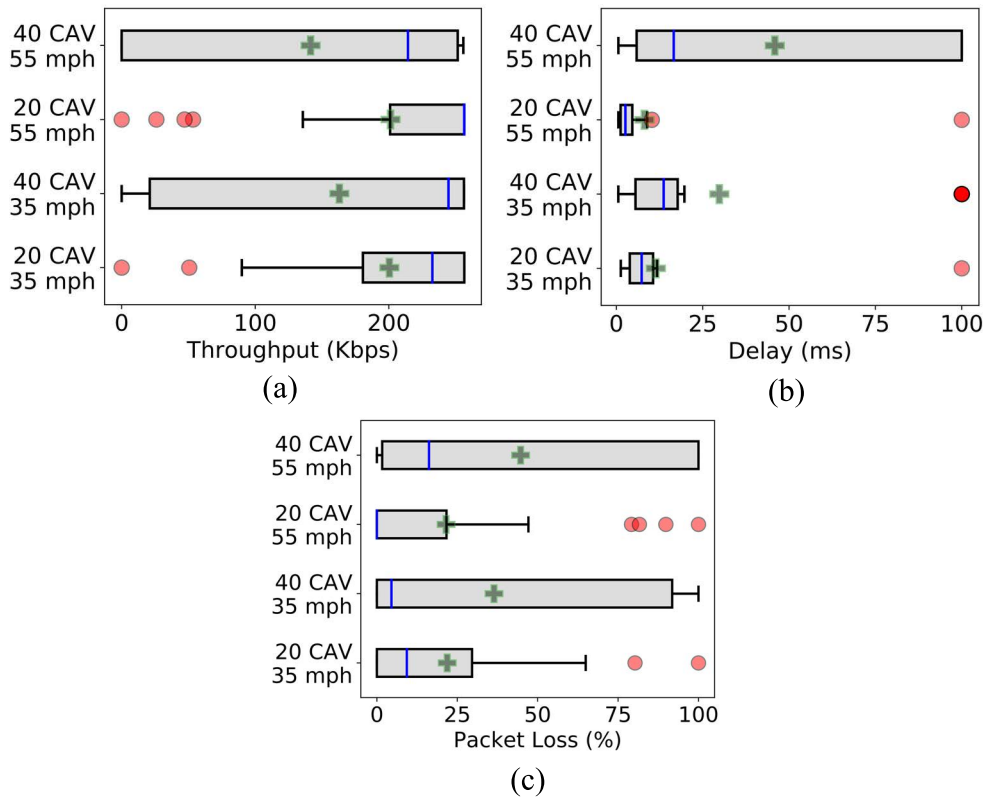


FIGURE 4. 5G mmWave performance for use case 2. (+ = sample mean): (a) throughput; (b) delay; and (c) packet loss.

- *timeLastRxPacket*: when the last packet in a flow was received
- *delaySum*: sum of all end-to-end delays for all received packets of a flow
- *txBytes*: total number of transmitted bytes for a flow
- *txPackets*: total number of transmitted packets for a flow
- *rxBytes*: total number of received bytes for a flow
- *rxPackets*: total number of received packets for a flow

Based on these output values for each flow, the performance evaluation metrics are calculated using the following equations, like the 5G mmWave scenarios.

- 1) **Average delay:** The average delay for each flow can be calculated using *delaySum* and *rxPackets* as given here.

$$Delay = \frac{delaySum}{rxPackets} \quad (4)$$

- 2) **Throughput:** Throughput for each flow can be calculated using *rxBytes*, *timeFirstTxPacket*, and *timeLastRxPacket*, as given below. We convert the total bytes received to bits and then measure the simulation time window by considering the timestamps for the first Tx packet and the last Rx packet.

$$Throughput = \frac{8rxBytes}{timeLastRxPacket - timeFirstTxPacket} \quad (5)$$

- 3) **Packet Loss:** Packet loss for each flow can be calculated using *txPackets* and *rxPackets*, as given below.

$$PacketLoss = \frac{txPackets - rxPackets}{txPackets} \quad (6)$$

VI. EXPERIMENTAL RESULTS

In this section, we discuss the findings based on the performance evaluation of the 5G mmWave and WAVE/IEEE 802.11p for three different use cases in a simulation environment.

A. USE CASE 1

In use case 1, the number of CVs is 20, the packet size is 1024 bytes, and the transmission (Tx) bit rate (i.e., data rate) is 250 Kbps. From Figure 3, we observe that the 5G mmWave performance is not affected by the maximum CV speed for the 20 CVs. The 5G mmWave eNB is able to provide average throughput of 200, 199 and 201 Kbps (see Figure 3(a)), average packet loss of 21.8%, 22.3% and 21.5% (see Figure 3(b)), an average delay of 6.5, 3.8 and 3.1 ms (see Figure 3(c)) for 35, 45 and 55 mph maximum speed of CVs, respectively. Although the delay is low, the packet loss is significant, resulting in low throughput. The WAVE/IEEE 802.11p suffers from significant delay and packet loss due to the throughput requirements from multiple CVs (see Figures 3(d) and 3(b)); this is due to the fact that WAVE/IEEE 802.11p has a maximum limit on the throughput

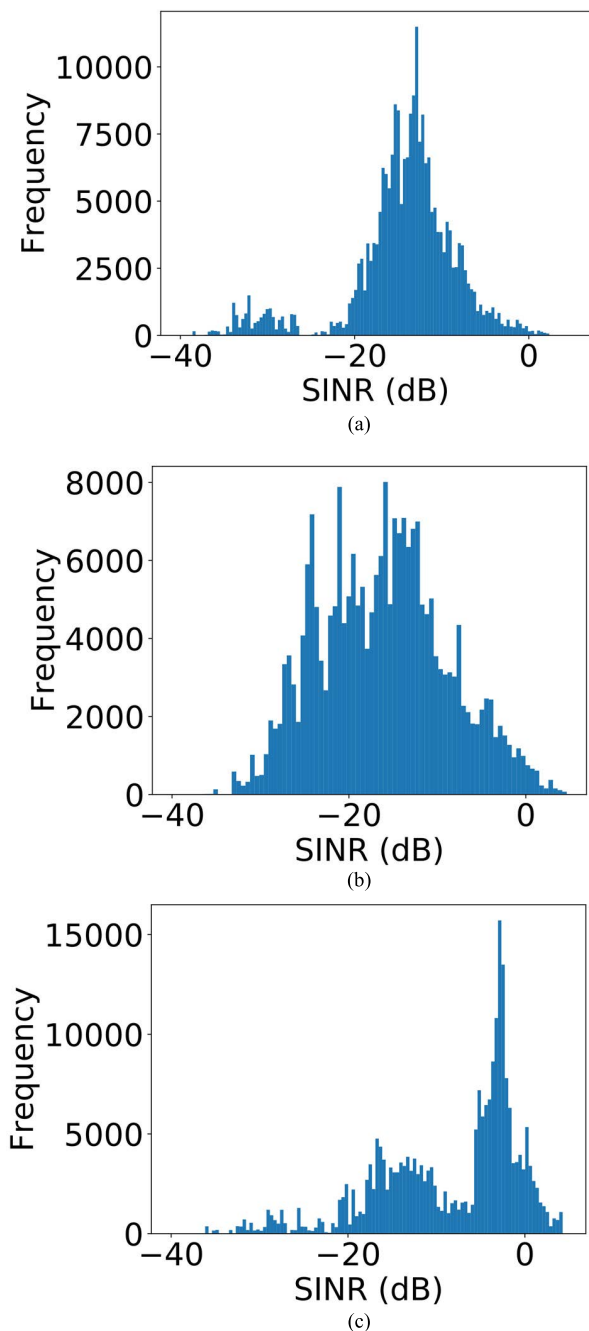


FIGURE 5. 5G mmWave SINR distribution variation with CV penetration level and V2I application data rate: (a) CV = 20, max speed = 45 mph, data rate = 250 Kbps; (b) CV = 40, max speed = 45 mph, data rate = 250 Kbps; and (c) CV = 20, max speed = 45 mph, data rate = 10 Mbps.

for UDP unicast transmission. For WAVE/IEEE 802.11p, the RSU can provide average throughput of 18, 46 and 14 Kbps (Figure 3(a)), average packet loss of 93.1%, 80.9% and 94.9% (see Figure 3(b)) and average delay of 2.8, 2.5 and 3.6 s (see Figure 3(d)) for 35, 45 and 55 mph speed of CVs, respectively. From these results, it can be concluded that even for low data rates, the 5G mmWave is superior to WAVE/IEEE 802.11p in terms of packet loss, throughput, and delay. Moreover, the impact of CV speed on the 5G mmWave is negligible for low penetration levels of CVs.

B. USE CASE 2

In use case 2, we investigate the combined effect of CV penetration level and CV mobility on communication performance. Here, we use two maximum speeds (35 mph and 55 mph) for CVs and two CV penetration levels (20 and 40 CVs). The packet size is 1024 bytes, and the Tx bit rate is 250 Kbps. From Figure 4, it can be observed that the CV penetration level has noticeable impacts on the performance of the 5G mmWave, regardless of the CV maximum speed. The increase in CV penetration level decreases the throughput and increases the delay and packet loss for both speeds. At 35 mph maximum speed, the 5G mmWave eNB can provide average throughput of 200 Kbps and 163 Kbps (as shown in Figure 4(a)), an average delay of 11.5 ms and 29.8 ms (see Figure 4(b)), and an average packet loss of 21.9% and 36.4% (see Figure 4(c)) for 20 and 40 CVs, respectively. At 55 mph maximum speed, the 5G mmWave eNB can provide average throughput of 201 and 141 Kbps (see Figure 4(a)), an average delay of 8.1 and 45.8 ms (see Figure 4(b)), and an average packet loss of 21.5% and 44.7% (see Figure 4(c)) for 20 and 40 CVs, respectively. Here, we can observe that doubling the number of CVs reduces the throughput by a factor ranging between 1.2 and 1.4, increases the average delay by factors ranging between 2.6 and 5.7, and increases packet loss by a factor ranging between 1.7 and 2.1. The increase in CVs increases the throughput requirements due to more applications downloading data using the 5G mmWave eNB. Moreover, more CVs in an urban area mean a higher probability of NLOS conditions [45], where any particular CV might be impeding the LOS of another CV. A scenario with a higher number of CVs also creates more multipath interference, which results in a higher loss of packets and end-to-end delays.

From the results in use case 1 (Figure 3), we have observed that the performance for 20 CVs remains unchanged for different speeds (35 mph, 45 mph, 55 mph). However, from Figure 4, we can observe that, for the 40 CV scenario, the 5G mmWave eNB performance degrades when the maximum speed is increased from 35 mph to 55 mph. The CVs' higher maximum speed also influences the 5G mmWave communication at higher CV penetration. For 20 CV scenarios, increasing the speed from 35 mph to 55 mph has no impact on the performance. However, for 40 CV scenarios, increasing the speed from 35 to 55 mph decreases the average throughput by a factor of 1.2 and increases the delay and packet loss by factors of 1.5 and 1.2, respectively. This is an interesting finding from use case 2, as it shows that the challenge factors are not independent. Instead, they can influence each other in affecting communication performance.

We have also measured the quality of the 5G mmWave communication in terms of SINR. SINR is a wireless quality indicator measured in decibels (dB). In a frequency distribution plot of SINR, a higher frequency at higher dB values represent better quality of wireless communication with higher throughput. Figures 5(a) and 5(b) show that interference and noise increase with the higher number of CVs. For CV = 20,

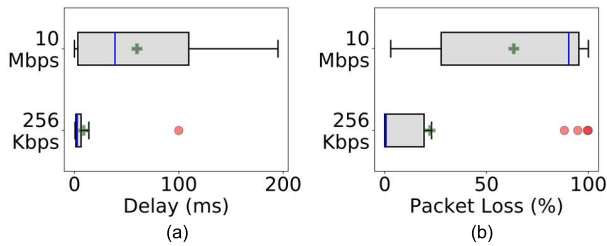


FIGURE 6. 5G mmWave performance for use case 3 (data rate). (+ = sample mean): (a) delay and (b) packet loss.

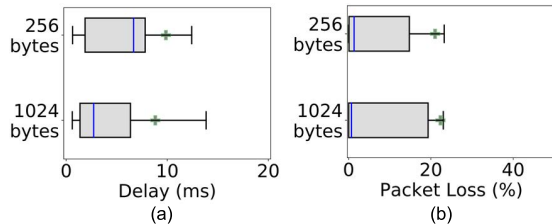


FIGURE 7. 5G mmWave performance for use case 3 (packet size) (+ = sample mean), (a) delay, (b) packet loss.

the SINR is mostly between -20 dB and 0 dB, but for $CV = 40$, the SINR is mostly spread out between 0 dB and -35 dB.

C. USE CASE 3

In use case 3, we examine the effect of V2I application specifications, specifically data rate and packet size, on the network performance of the 5G mmWave. At first, we investigated the effect of higher data rates on the performance of the 5G mmWave. Thus, we increase the data rate from 250 Kbps to 10 Mbps for each CV, keeping the packet size fixed at 1024 bytes. In this case, we use 20 CVs at an average speed of 45 mph. From Figure 6, we observe that a higher bit rate has a noticeable impact on network performance. The average throughput is higher because of the higher Tx bit rate. We have found that for the 10 Mbps case, the average delay is 59.9 ms compared to the 8.8 ms for the 250 Kbps case, so the delay increases by a factor of 6.8 when the bit rate increases by a factor of 40 (Figure 6(a)). The average packet loss increases from 22.3% (for the 250 Kbps case) to 63.3% (for the 10 Mbps case), which is an increase by a factor of 2.8 (Figure 6(b)).

We examine the effect of packet size on the network performance of the 5G mmWave by decreasing the packet size from 1024 bytes to 256 bytes for each CV, keeping the data rate fixed at 250 Kbps. For this case, we use 20 CVs at an average speed of 45 mph. From Figure 7, we observe that a change in packet size has no significant impact on the delay (Figure 7(a)) and packet loss (Figure 7(b)). The average delay is 9.8 ms compared to the 8.8 ms for the 1024 bytes case, and the average packet loss is 21% compared to 22.3% for the 1024 bytes case.

As shown in Figure 5(c), the SINR distribution is improved compared to Figures 5(a) and 5(b) due to the higher Tx bit rate and higher throughput. Throughput is logarithmically proportional to SINR, as defined by the Shannon-Hartley theorem [46].

VII. CONCLUSION

Based on the results presented in Section VI, the CV penetration level, dynamic mobility, and application data rate have noticeable impacts on the performance of the 5G mmWave. Our analysis has revealed that doubling the CV penetration level reduces the throughput by a factor ranging between 1.2 and 1.4, increases the average delay by factors ranging between 2.6 and 5.7, and increases packet loss by a factor ranging between 1.7 and 2.1. Moreover, for a higher CV penetration level, CV speed has an impact on network performance. However, this impact is not present for the lower CV penetration level. The CV application data rate also has a significant impact on the performance. For an increase in data rate by a factor of 40, the average delay increases by a factor of 6.8, whereas the average packet loss increases by a factor of 2.8. Changing the packet size does not have any impact on the delay, packet loss, and throughput. Also, we find higher noise and interference when the CV penetration level increases and the data rate increases, leading to network performance degradation. The potential solutions for supporting CV applications may include deploying multiple 5G mmWave base stations or leveraging existing 5G base stations.

VIII. RECOMMENDATIONS FOR FUTURE RESEARCH

Our recommendations for future research are divided into two subsections: simulation and field evaluations.

A. SIMULATION-BASED RESEARCH

This study does not consider the effects of buildings and blockages on the 5G mmWave communication. It only shows the 5G mmWave's performance in the line-of-sight or LOS scenario. The 5G mmWave signals are susceptible to signal blockage and non-line-of-sight or NLOS. Future research should focus on simulating different types of scenarios considering buildings and blockages (e.g., urban roadway tunnels, rural areas) to investigate their effect on the performance of the 5G mmWave.

In this study, we have simulated a limited number of CVs on the road. Future studies should investigate a larger area with a higher number of CVs. These future case studies can identify the shortcomings in 5G mmWave communication with a higher penetration of CVs in urban networks and could point towards further improvements in the 5G mmWave technology. We have simulated a portion of a corridor (~ 500 m) and the performance of one 5G mmWave base station for this particular area. Future research should investigate multiple 5G mmWave base stations' performance, different spacing between the base stations, and intelligent handoff management for CVs to perform horizontal handover between the base stations. A heterogeneous network with the 5G mmWave and other communication technology (e.g., 4G, LTE, DSRC, and WiFi) provides a reliable communication system for an extended travel area, such as intercity highways. CVs will perform vertical handover between these communication technologies based on their availability and coverage.

B. FIELD EVALUATION

A part of the 5G rollout nationally includes mmWave base station deployments, especially in urban areas with high user density. Therefore, along with detailed sensitivity analysis through simulations, the 5G mmWave should also be evaluated using field tests in urban areas containing many users. The evaluation may include the validation of simulation results and updating simulation parameters. A connected vehicle testbed containing the 5G mmWave base stations will be ideal for conducting further research and evaluating communication performance. Finally, we should develop testbeds having the 5G mmWave base stations to test different CV (V2V and V2I) applications.

ACKNOWLEDGMENT

This work was supported by the Center for Connected Multimodal Mobility (C^2M^2) (the U.S. Department of Transportation Tier 1 University Transportation Center) headquartered at Clemson University, Clemson, SC, USA. However, the U.S. Government assumes no liability for the contents or use thereof.

REFERENCES

- [1] USDOT. *Architecture Reference for Cooperative and Intelligent Transportation*. ARC-IT. Accessed: Apr. 14, 2021. [Online]. Available: <https://local.iteris.com/arc-it/>
- [2] D. Roy, M. Chatterjee, and E. Pasilio, "Video quality assessment for inter-vehicular streaming with IEEE 802.11p, LTE, and LTE direct networks over fading channels," *Comput. Commun.*, vol. 118, pp. 69–80, Mar. 2018, doi: [10.1016/j.comcom.2017.09.010](https://doi.org/10.1016/j.comcom.2017.09.010).
- [3] T. S. Rappaport, G. R. MacCartney, Jr., S. Sun, H. Yan, and S. Deng, "Small-scale, local area, and transitional millimeter wave propagation for 5G communications," *IEEE Trans. Antennas Propag.*, vol. 65, no. 12, pp. 6474–6490, Nov. 2017, doi: [10.1109/TAP.2017.2734159](https://doi.org/10.1109/TAP.2017.2734159).
- [4] I. Mavromatis, A. Tassi, R. J. Piechocki, and A. Nix, "Efficient V2 V communication scheme for 5G mmWave hyper-connected CAVs," in *Proc. IEEE Int. Conf. Commun. Workshops (ICC Workshops)*, May 2018, pp. 1–6, doi: [10.1109/ICCWorkshops.2018.8403780](https://doi.org/10.1109/ICCWorkshops.2018.8403780).
- [5] I. Rasheed and F. Hu, "Intelligent super-fast vehicle-to-everything 5G communications with predictive switching between mmWave and THz links," *Veh. Commun.*, vol. 27, Jan. 2021, Art. no. 100303, doi: [10.1016/j.vehcom.2020.100303](https://doi.org/10.1016/j.vehcom.2020.100303).
- [6] Y. Li, C.-Y.-D. Sim, Y. Luo, and G. Yang, "12-port 5G massive MIMO antenna array in sub-6GHz mobile handset for LTE bands 42/43/46 applications," *IEEE Access*, vol. 6, pp. 344–354, 2017, doi: [10.1109/ACCESS.2017.2763161](https://doi.org/10.1109/ACCESS.2017.2763161).
- [7] P. Adhikari. (2008). *Understanding Millimeter Wave Wireless Communication*. Loea Corporation. Accessed: Sep. 9, 2021. [Online]. Available: <https://www.semanticscholar.org/paper/Understanding-Millimeter-Wave-Wireless-Adhikari/540ad9ad8412733dd235715be44f978434164da9>
- [8] M. Xiao, S. Mumtaz, Y. Huang, L. Dai, Y. Li, M. Matthaiou, G. K. Karagiannidis, E. Björnson, K. Yang, and I. Chih-Lin, "Millimeter wave communications for future mobile networks," *IEEE J. Sel. Areas Commun.*, vol. 35, no. 9, pp. 1909–1935, Sep. 2017, doi: [10.1109/JSAC.2017.2719924](https://doi.org/10.1109/JSAC.2017.2719924).
- [9] I. Rasheed, F. Hu, Y.-K. Hong, and B. Balasubramanian, "Intelligent vehicle network routing with adaptive 3D beam alignment for mmWave 5G-based V2X communications," *IEEE Trans. Intell. Transp. Syst.*, vol. 22, no. 5, pp. 2706–2718, May 2021, doi: [10.1109/TITS.2020.2973859](https://doi.org/10.1109/TITS.2020.2973859).
- [10] C. Storck and F. Duarte-Figueiredo, "A 5G V2X ecosystem providing internet of vehicles," *Sensors*, vol. 19, no. 3, p. 550, Jan. 2019, doi: [10.3390/s19030550](https://doi.org/10.3390/s19030550).
- [11] J. Hu, C. Chen, T. Qiu, and Q. Pei, "Regional-centralized content dissemination for eV2X services in 5G mmWave-enabled IoV," *IEEE Internet Things J.*, vol. 7, no. 8, pp. 7234–7249, Aug. 2020, doi: [10.1109/JIOT.2020.2982983](https://doi.org/10.1109/JIOT.2020.2982983).
- [12] R. He, C. Schneider, B. Ai, and G. Wang, "Propagation channels of 5G millimeter-wave vehicle-to-vehicle communications: Recent advances and future challenges," *IEEE Veh. Technol. Mag.*, vol. 15, no. 1, pp. 16–26, Mar. 2020, doi: [10.1109/MVT.2019.2928898](https://doi.org/10.1109/MVT.2019.2928898).
- [13] A. Bohli and R. Buallegue, "How to meet increased capacities by future green 5G networks: A survey," *IEEE Access*, vol. 7, pp. 42220–42237, 2019, doi: [10.1109/ACCESS.2019.2907284](https://doi.org/10.1109/ACCESS.2019.2907284).
- [14] K. C. Dey, A. Rayamajhi, M. Chowdhury, P. Bhavsar, and J. Martin, "Vehicle-to-vehicle (V2V) and vehicle-to-infrastructure (V2I) communication in a heterogeneous wireless network—Performance evaluation," *Transp. Res. C, Emerg. Technol.*, vol. 68, pp. 168–184, Jul. 2016, doi: [10.1016/j.trc.2016.03.008](https://doi.org/10.1016/j.trc.2016.03.008).
- [15] A. S. Huang, M. Antone, E. Olson, L. Fletcher, D. Moore, S. Teller, and J. Leonard, "A high-rate, heterogeneous data set from the DARPA urban challenge," *Int. J. Robot. Res.*, vol. 29, no. 13, pp. 1595–1601, Nov. 2010, doi: [10.1177/0278364910384295](https://doi.org/10.1177/0278364910384295).
- [16] D. Brake. (Apr. 2020). *A U.S. National Strategy for 5G and Future Wireless Innovation*. Information Technology and Innovation Foundation. Accessed: Sep. 9, 2021. [Online]. Available: <https://itif.org/publications/2020/04/27/us-national-strategy-5g-and-future-wireless-innovation>
- [17] P. Datta and S. Kaushal, "Exploration and comparison of different 4G technologies implementations: A survey," in *Proc. Recent Adv. Eng. Comput. Sci. (RAECS)*, Mar. 2014, pp. 1–6, doi: [10.1109/RAECS.2014.6799517](https://doi.org/10.1109/RAECS.2014.6799517).
- [18] S. Ahmadi, *5G NR—Architecture, Technology, Implementation, and Operation of 3GPP New Radio Standards*, 1st ed. New York, NY, USA: Academic, 2019.
- [19] D. Garcia-Roger, E. E. Gonzalez, D. Martin-Sacristan, and J. F. Monserrat, "V2X support in 3GPP specifications: From 4G to 5G and beyond," *IEEE Access*, vol. 8, pp. 190946–190963, 2020, doi: [10.1109/ACCESS.2020.3028621](https://doi.org/10.1109/ACCESS.2020.3028621).
- [20] N. Loulloudes, G. Pallis, and M. D. Dikaiakos, "The dynamics of vehicular networks in urban environments," 2010, *arXiv:1007.4106*. Accessed: Sep. 9, 2021. [Online]. Available:
- [21] M. Sepulcre, J. Mittag, P. Santi, H. Hartenstein, and J. Gozalvez, "Congestion and awareness control in cooperative vehicular systems," *Proc. IEEE*, vol. 99, no. 7, pp. 1260–1279, Jul. 2011, doi: [10.1109/JPROC.2011.2116751](https://doi.org/10.1109/JPROC.2011.2116751).
- [22] R. Stanica, E. Chaput, and A.-L. Beylot, "Local density estimation for contention window adaptation in vehicular networks," in *Proc. IEEE 22nd Int. Symp. Pers., Indoor Mobile Radio Commun.*, Sep. 2011, pp. 730–734, doi: [10.1109/PIMRC.2011.6140062](https://doi.org/10.1109/PIMRC.2011.6140062).
- [23] M. Afaq, J. Iqbal, T. Ahmed, I. Ul Islam, M. Khan, and M. S. Khan, "Towards 5G network slicing for vehicular ad-hoc networks: An end-to-end approach," *Comput. Commun.*, vol. 149, pp. 252–258, Jan. 2020, doi: [10.1016/j.comcom.2019.10.018](https://doi.org/10.1016/j.comcom.2019.10.018).
- [24] C. Dehos, J. L. González, A. De Domenico, D. Kténas, and L. Dussot, "Millimeter-wave access and backhauling: The solution to the exponential data traffic increase in 5G mobile communications systems?" *IEEE Commun. Mag.*, vol. 52, no. 9, pp. 88–95, Sep. 2014, doi: [10.1109/MCOM.2014.6894457](https://doi.org/10.1109/MCOM.2014.6894457).
- [25] A. Mastro Simone and D. Panno, "A comparative analysis of mmWave vs LTE technology for 5G moving networks," in *Proc. IEEE 11th Int. Conf. Wireless Mobile Comput., Netw. Commun. (WiMob)*, Oct. 2015, pp. 422–429, doi: [10.1109/WiMob.2015.7347993](https://doi.org/10.1109/WiMob.2015.7347993).
- [26] M. Mezzavilla, M. Zhang, M. Polese, R. Ford, S. Dutta, S. Rangan, and M. Zorzi, "End-to-end simulation of 5G mmWave networks," *IEEE Commun. Surveys Tuts.*, vol. 20, no. 3, pp. 2237–2263, 3rd Quart., 2018, doi: [10.1109/COMST.2018.2828880](https://doi.org/10.1109/COMST.2018.2828880).
- [27] M. Giordani, A. Zanella, and M. Zorzi, "Technical report—millimeterwave communication in vehicular networks: Coverage and connectivity analysis," Apr. 2017, *arXiv:1705.06960*. Accessed: Oct. 27, 2021.
- [28] F. Arena, G. Pau, and A. Severino, "A review on IEEE 802.11p for intelligent transportation systems," *J. Sensor Actuator Netw.*, vol. 9, no. 2, p. 22, Apr. 2020, doi: [10.3390/jsan9020022](https://doi.org/10.3390/jsan9020022).
- [29] SAE. (2021). *Vehicle Safety Communications Landscape Clarifies With Controversial FCC Ruling*. SAE Internationals. Accessed: Sep. 10, 2021. [Online]. Available: <https://www.sae.org/site/news/2020/11/fcc-5.9-ghz-cv2x-decision>
- [30] V. Mannoni, V. Berg, S. Sesia, and E. Perraud, "A comparison of the V2X communication systems: ITS-G5 and C-V2X," in *Proc. IEEE 89th Veh. Technol. Conf. (VTC-Spring)*, Apr. 2019, pp. 1–5, doi: [10.1109/VTC-Spring.2019.8746562](https://doi.org/10.1109/VTC-Spring.2019.8746562).
- [31] G. Carneiro. (2010). *NS-3: Network Simulator 3*. Accessed: Mar. 5, 2022. [Online]. Available: <https://www.nsnam.org/tutorials/NS-3-LABMEETING-1.pdf>

- [32] M. Behrisch, L. Bieker, J. Erdmann, and D. Krajzewicz, "SUMO—simulation of urban mobility: An overview," in *Proc. 3rd Int. Conf. Adv. Syst. Simulation (SIMUL)*, 2011, pp. 63–68.
- [33] N. Baldo. (2011). *The NS-3 LTE Module by the LENA Project*. Accessed: Mar. 5, 2022. [Online]. Available: <https://www2.nsnam.org/tutorials/tutorials/consortium13/lte-tutorial.pdf>
- [34] F. Van den Abeele, J. Haxhibeqiri, I. Moerman, and J. Hoebeke, "Scalability analysis of large-scale LoRaWAN networks in ns-3," *IEEE Internet Things J.*, vol. 4, no. 6, pp. 2186–2198, Dec. 2017, doi: [10.1109/JIOT.2017.2768498](https://doi.org/10.1109/JIOT.2017.2768498).
- [35] Z. Hossain, Q. Xia, and J. M. Jornet, "Terasim: An NS-3 extension to simulate terahertz-band communication networks," *Nano Commun. Netw.*, vol. 17, pp. 36–44, Sep. 2018, doi: [10.1016/j.nancom.2018.08.001](https://doi.org/10.1016/j.nancom.2018.08.001).
- [36] M. R. Akdeniz, Y. Liu, M. K. Samimi, and S. Sun, "Millimeter wave channel modeling and cellular capacity evaluation," *IEEE J. Sel. Areas Commun.*, vol. 32, no. 6, pp. 1164–1179, Jun. 2014, doi: [10.1109/JSAC.2014.2328154](https://doi.org/10.1109/JSAC.2014.2328154).
- [37] R. Chitraxi, U. Upadhyaya, T. Makwana, and P. Mahida, "Simulation of VANET using NS-3 and SUMO," *Int. J. Adv. Res. Comput. Sci. Softw. Eng.*, vol. 4, no. 4, pp. 563–569, 2014.
- [38] NS-3. *VANET-Routing-Compare.CC*. Accessed: Jan. 11, 2022. [Online]. Available: https://www.nsnam.org/doxygen/vanet-routing-compare_8cc_source.html
- [39] Z. H. Mir and F. Filali, "On the performance comparison between IEEE 802.11p and LTE-based vehicular networks," in *Proc. IEEE 79th Veh. Technol. Conf. (VTC Spring)*, May 2014, pp. 1–5, doi: [10.1109/VTC-Spring.2014.7023017](https://doi.org/10.1109/VTC-Spring.2014.7023017).
- [40] S. Kumar, A. Kumar, V. Tyagi, and A. Kumar, "Impact of network density on AODV protocol in VANET," in *Proc. IEEE 5th Int. Conf. Comput. Commun. Autom. (ICCCA)*, Greater Noida, India, Oct. 2020, pp. 559–564, doi: [10.1109/ICCCA49541.2020.9250898](https://doi.org/10.1109/ICCCA49541.2020.9250898).
- [41] S. Hosmani and B. Mathapati, "Efficient vehicular ad hoc network routing protocol using weighted clustering technique," *Int. J. Inf. Technol.*, vol. 13, no. 2, pp. 469–473, Apr. 2021, doi: [10.1007/s41870-020-00537-2](https://doi.org/10.1007/s41870-020-00537-2).
- [42] A. Ahamed, "Improving routing protocols to enhance QoS in VANET," Ph.D. dissertation, Univ. Nebraska-Lincoln, Lincoln, NE, USA, 2021. Accessed: Mar. 4, 2022. [Online]. Available: <https://www.proquest.com/docview/2572581098/abstract/B175AD26B00D476APQ/1>
- [43] B. S. Yelure and S. P. Sonavane, "QoS evaluation of VANET routing protocol," in *Proc. Int. Conf. Commun. Electron. Syst. (ICCES)*, Jul. 2019, pp. 813–818, doi: [10.1109/ICCES45898.2019.9002115](https://doi.org/10.1109/ICCES45898.2019.9002115).
- [44] G. Carneiro, P. Fortuna, and M. Ricardo, "FlowMonitor: A network monitoring framework for the network simulator 3 (NS-3)," in *Proc. 4th Int. ICST Conf. Perform. Eval. Methodol. Tools*, Brussels, Belgium, Oct. 2009, pp. 1–10, doi: [10.4108/ICST.VALUETOOLS2009.7493](https://doi.org/10.4108/ICST.VALUETOOLS2009.7493).
- [45] L. Montero, C. Ballesteros, C. de Marco, and L. Jofre, "Beam management for vehicle-to-vehicle (V2 V) communications in millimeter wave 5G," *Veh. Commun.*, vol. 34, Apr. 2022, Art. no. 100424, doi: [10.1016/j.vehcom.2021.100424](https://doi.org/10.1016/j.vehcom.2021.100424).
- [46] C. E. Shannon, "A mathematical theory of communication," *ACM SIG-MOBILE Mobile Comput. Commun. Rev.*, vol. 5, no. 1, pp. 3–55, 2001, doi: [10.1145/584091.584093](https://doi.org/10.1145/584091.584093).



ZADID KHAN received the B.Sc. degree in electrical and electronic engineering from the Bangladesh University of Engineering and Technology (BUET), Dhaka, Bangladesh, in 2014, and the M.Sc. and Ph.D. degrees in civil engineering (transportation major) from Clemson University, Clemson, SC, USA, in 2018 and 2021, respectively. From 2014 to 2016, he served as a Petroleum Engineer for the Asset Development Department, Chevron Bangladesh Profit Center (BPC). He is currently working as a Senior Data Analyst in supply chain (transportation) with Walmart Inc. During his M.Sc. and Ph.D. degrees, he worked with the Cyber Physical Systems (CPS) Laboratory as a Graduate Research Assistant, under the supervision of Dr. Mashrur Chowdhury, Professor, Department of Civil Engineering. His primary research interests include transportation cyber physical systems, connected and autonomous vehicles, and data analytics for transportation. Within these domains, his research interests include data science (machine/deep learning), computer communication and networking, data analytics (data mining, data fusion, big data, and data visualization), cloud computing, cybersecurity, and optimization.



SAKIB MAHMUD KHAN (Senior Member, IEEE) received the M.Sc. and Ph.D. degrees in civil engineering from Clemson University, in 2015 and 2019. He currently holds a joint appointment at Clemson University as the Assistant Director of the Center for Connected Multimodal Mobility (C²M², a Tier 1 USDOT University Transportation Center), and as an Assistant Research Professor with the School of Civil and Environmental Engineering and Earth Sciences. Before joining C²M², he was a Postdoctoral Research Scholar working at the University of California at Berkeley, Berkeley, CA, USA. He is the Manager of the Clemson Smart City Testbed. His research interests include both theoretical and applied aspects of artificial intelligence, optimization, and traffic-flow theory. His research application areas include transportation cyber-physical-social systems, connected and autonomous vehicles in the Internet of Things environment, heterogeneous wireless communications, transportation cybersecurity and privacy, quantum cloud-edge collaboration, and transportation big data analytics.



MASHRUR CHOWDHURY (Senior Member, IEEE) received the Ph.D. degree in civil engineering from the University of Virginia, USA, in 1995. Prior to entering academia in August 2000, he was a Senior ITS Systems Engineer with Iteris Inc. and a Senior Engineer with Bellomo–McGee Inc., where he served as a Consultant to many state and local agencies, and the U.S. Department of Transportation on ITS related projects. He is currently the Eugene Douglas Mays Chair of Transportation with the Glenn Department of Civil Engineering, Clemson University, Clemson, SC, USA. He is the Director of the USDOT Center for Connected Multimodal Mobility (a TIER 1 USDOT University Transportation Center). He is the Co-Director of the Complex Systems, Data Analytics and Visualization Institute (CSAVI), Clemson University. He is also the Director of the Transportation Cyber-Physical-Social Systems Laboratory, Clemson University. He is a fellow of the American Society of Civil Engineers. He serves as an Associate Editor for the IEEE TRANSACTIONS ON INTELLIGENT TRANSPORTATION SYSTEMS. He is a Registered Professional Engineer in OH, USA.



MIZANUR RAHMAN (Member, IEEE) received the M.Sc. and Ph.D. degrees in civil engineering (transportation systems) from Clemson University, in 2013 and 2018, respectively. After his graduation in August 2018, he joined as a Postdoctoral Research Fellow with the Center for Connected Multimodal Mobility (C²M²), the U.S. Department of Transportation Tier 1 University Transportation Center (ccas.clemson.edu/c2m2). After that, he worked as an Assistant Director of the C²M². He is currently an Assistant Professor with the Department of Civil, Construction and Environmental Engineering, University of Alabama, Tuscaloosa, AL, USA. He was closely involved in the development of South Carolina Connected Vehicle Testbed (SC-CVT). His research interests include traffic flow theory, and transportation cyber-physical systems for connected and automated vehicles and smart cities.



MHAFUZUL ISLAM received the B.S. degree in computer science and engineering from the Bangladesh University of Engineering and Technology (BUET), in 2014, and the M.S. and Ph.D. degrees in civil engineering from Clemson University, in 2018 and 2021, respectively. He is currently working as a Senior Researcher at General Motors. His research interests include transportation cyber-physical systems with an emphasis on data-driven connected and autonomous vehicle.

• • •